

## Validation of a mesoscale hydrological model in a small-scale forested catchment

Václav Šípek and Miroslav Tesař

### ABSTRACT

The aim of this study was to examine the abilities of the mesoscale ecohydrological model Soil And Water Integrated Model (SWIM) to simulate discharge, soil moisture, and groundwater dynamics in a small-scale forested catchment. Moreover, the influence of two lateral flow computation techniques on the simulation efficiency was assessed. Generally, the discharges were simulated poorly. Groundwater level was estimated reasonably taking into account that the model was not designed for small-scale catchments. The soil moisture simulation exhibited good correspondence with the observed data in the warmer season (April–August). Both the dynamics and the magnitude were estimated sufficiently well. On the other hand, the colder season does not comply satisfactorily with the modelled data, as the decline of moisture content (in the non-precipitation periods) has no model response. The kinematic storage method was found to be more reliable in the case of a small-scale forested catchment compared to the exponential storage lateral flow estimation approach.

**Key words** | hydrological modelling, small catchment, soil moisture, subsurface lateral flow, SWIM

Václav Šípek (corresponding author)

Miroslav Tesař

The Institute of Hydrodynamics of the Academy of Sciences of the Czech Republic,

Pod Patankou 30/5,

Prague 166 12,

Czech Republic

E-mail: [sipek@ih.cas.cz](mailto:sipek@ih.cas.cz)

### INTRODUCTION

Soil moisture plays a key role in the hydrological cycle and also in the entire ecosystem. It controls the flux of water between soil, vegetation, and atmosphere. As the water cycle is subjected to various stresses, there is a need for an estimation of the impacts of these stresses on the soil moisture regime. The reason is that the volume of water stored within the soil has a direct effect on vegetation growth, crop yield, and, in particular, the volume and timing of runoff. Several studies have indicated the important consequences of soil moisture deficit within catchments (Entin *et al.* 2000; Daly & Porporato 2005). Hence, understanding of soil moisture variability is important for the modelling of the climate system and improves hydrological simulation. It also provides the background for hydrological forecasting systems as antecedent moisture conditions and their patterns represent crucial parameters.

Recently, mesoscale hydrological models have been widely applied for estimating not only the discharge, but also the nutrient dynamics and the complex influence of climate change on various catchments (Ficklin *et al.* 2009; Huang *et al.* 2009). These models are considered to be appropriate

for simulations of the hydrological cycle in mesoscale (ranging from 100 to 10,000 km<sup>2</sup>) and macroscale (> 10,000 km<sup>2</sup>) areas. However, the application of these types of models at larger scale is based on the assumption that they are able to predict the particular components of the hydrological cycle in a reasonable way. This assumption can be efficiently validated only at the small scale as the required data are usually not available for larger areas. The hydrological models Soil and Water Assessment Tool (SWAT) and Soil and Water Integrated Model (SWIM) represent the aforementioned type of models and have very similar components concerning the modelling of the hydrological cycle (Krysanova *et al.* 2005). The mesoscale ecohydrological model SWIM was chosen in this study as a tool for hydrological modelling.

SWIM has already been used for a number of studies investigating the impact of climate or land-use changes on the hydrological cycle (Holsten *et al.* 2009; Nemeckova *et al.* 2011), nutrient dynamics (Hesse *et al.* 2008; Huang *et al.* 2009), and crop yield (Krysanova *et al.* 2005). The performance of the SWAT/SWIM type of model with regard to

discharge at the macroscale was verified by several authors (e.g. Srinivasan *et al.* 1998; Hattermann *et al.* 2005; Koch *et al.* 2013). However, the SWAT/SWIM type of model was originally designed for rural areas (Arnold *et al.* 1993). Nevertheless, using this type of model for meso- and macro-scale tasks (where detailed measurements are not available) means that certain parts of the landscape are usually covered by forest. Hence, the assessment of the model's performance in a small-scale forested catchment is a valuable source of information for modellers using this type of model in areas with diverse land cover.

A number of the existing models such as *Système Hydrologique Européen Model* (e.g. Abbott *et al.* 1986), *TOPMODEL* (Beven & Kirkby 1979), *SWAT* (Arnold *et al.* 1993), and *SWIM* (Krysanova *et al.* 1998, 2005), which operate at the larger scale, use different methods for the soil moisture estimation. In spite of numerous applications of models of the SWAT/SWIM type, only a few contributions have dealt explicitly with soil moisture (DeLiberty & Legates 2003; Holsten *et al.* 2009; Li *et al.* 2010). These studies are primarily focussed on average monthly soil moisture values or trend analysis in modelled datasets. Thus, a reliable evaluation of this model component concerning the daily soil moisture records in both the vegetation season and the dormant season is missing. This is especially important when the SWAT/SWIM type of model is used for large-scale analysis of climate or land-use change in various components of the hydrological cycle (Ficklin *et al.* 2009; Huang *et al.* 2010) or, for example, to validate a satellite-based estimation of actual evapotranspiration (Fang *et al.* 2012).

The primary motivation for this experiment originates in the need to establish a modelling scheme that would enable reliable year-round soil moisture content estimation in mesoscale catchments with diverse land cover. This might be further used for the improvement of impact studies (climate and land-use change, agricultural management) on the hydrological regime and also for more accurate determination of the moisture saturation level of various regions, which is necessary for hydrological forecasting systems.

Thus, the main aims of this study are:

- to assess the ability of the mesoscale SWIM model to simulate the rainfall–runoff relation in a small-scale forested catchment (0.99 km<sup>2</sup>);

- to investigate the reliability of soil water content and groundwater level simulations;
- to assess the influence of two different approaches of lateral subsurface flow estimation (kinematic and exponential storage) on discharge, soil moisture, and groundwater level simulations.

## METHODS USED AND DATA PROCESSING

### Study area and data

The small-scale experimental Liz catchment (13° 41' E, 49° 04' N) is located in the mountainous part of the Czech Republic and covers 99.7 ha (Figure 1). The soil type is determined by the geologic base and can be classified as moderately deep sandy loam acidic podzols. The soil profile can be schematized into three soil horizons: 0–17, 17–60, and 60–100 cm (Tesar *et al.* 2001). As the catchment spreads along a forested hillslope, the soil has generally good water permeability (saturated hydraulic conductivity ranges from 200 to 350 mm/hr). Hence, surface runoff has been observed very rarely (usually caused by extreme rainfall of the order of hundreds of millimetres per couple of days). The altitude of the catchment starts at 828 m.a.s.l. (the outlet) and reaches 1,074 m.a.s.l. (the surrounding peaks). Climate and vegetation are characteristic for the mild climate zone, with the mean monthly temperature varying from –3.4 °C in January to 13.6 °C in July. The average annual temperature is 6.3 °C. The average annual precipitation attains 825 mm, with summer being the most humid period (June–August, with approximately one-third of the annual precipitation). According to the long-term water balance, the annual actual evapotranspiration is around 500 mm/year. The entire catchment is covered by mixed forest, with prevailing coniferous trees of various ages (up to 140 years).

The meteorological data necessary to run the model were obtained from the meteorological station located next to the experimental catchment (330 m from its border and 1,000 m from the centre of the catchment) at the altitude of 830 m.a.s.l. It is located on the meadow and thus records open rainfall without the influence of interception losses. Hence, the station is considered to be representative. The

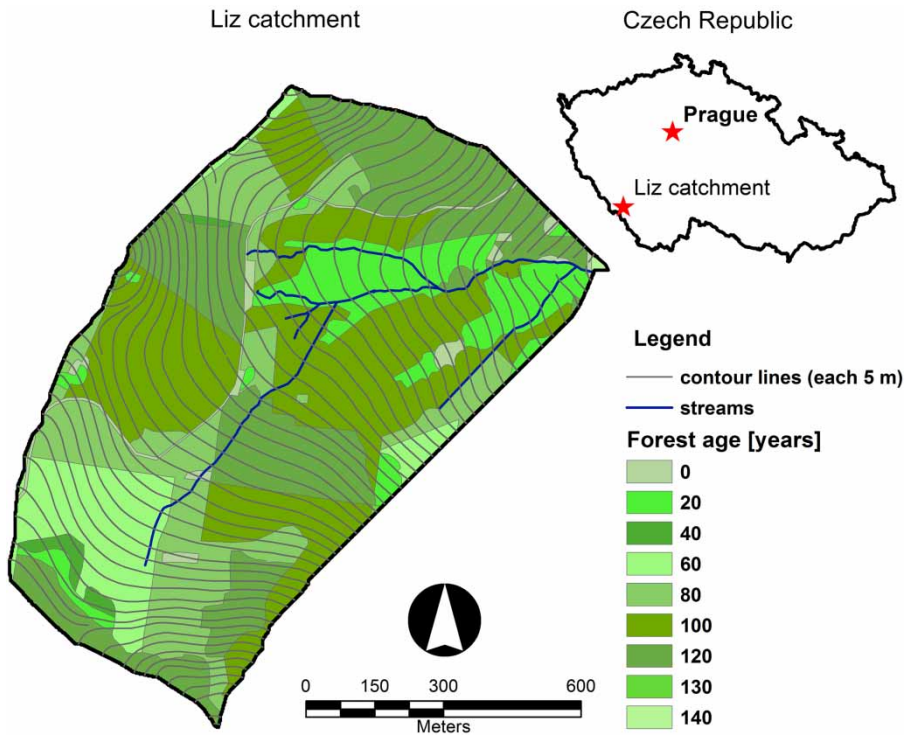


**Figure 1** | Study site location and overview map of the Liz catchment with forest age shown.

datasets consist of precipitation, air temperature, air relative humidity, and solar radiation records from the period of 2007–2010. The water level is measured by the ultrasonic probe in the catchment's closing profile and the long-term average is equal to  $0.011 \text{ m}^3 \text{ s}^{-1}$  (1975–2010).

The suction pressure of soil water was measured by a set of tensiometers (UMS T8) at three depths (15, 40, and 60 cm). As these data were available from July 2008, the study deals with 2 subsequent years (2009–2010), in which only 2 days of measurements are missing. The precise location of the soil moisture measurement was chosen in order to represent the average age of the forest, the average hillslope angle, and approximately average altitude within the catchment. The soil moisture content was derived from suction pressure using a retention curve proposed by Van Genuchten (1980). The exact parameters of the retention curves are displayed in Table 1.

The groundwater level has been measured manually once a week by the acoustic device in a borehole since 1976. For the purpose of groundwater level monitoring, a network of four boreholes was created. For this study, the borehole near the closing profile of the Liz experimental

**Table 1** | Parameters of van Genuchten expression of retention curves for three depths

	Depth		
	15 cm	40 cm	60 cm
$\theta_r$ [%]	0.00	0.17	0.16
$\theta_s$ [%]	0.73	0.53	0.50
$\alpha$ [-]	0.09	0.05	0.06
$n$ [-]	1.19	1.60	1.47

$\theta_r$  and  $\theta_s$  – residual and saturated volumetric water contents, respectively;  $\alpha$  and  $n$  – shape parameters of the retention curve.

catchment was chosen. This borehole has an inner diameter of 150 mm and depth of 12 m, and the groundwater level of the unconfined aquifer ranges from 1.7 to 8.2 m from the ground surface.

Four layers of spatial data are necessary for the hydrological model: a subbasin map, a digital elevation model, a soil map, land cover characteristics, and optionally a map of the river network. The subbasin map was derived by the model's MapWindow interface from the digital elevation model (Czech Geodesy Agency). Land cover data were extracted from the CORINE land cover database, and the soil map

(Nemeckova 2008) was created based on the experimental datasets from the Czech University of Life Sciences.

### Ecohydrological model SWIM

The ecohydrological model SWIM is a continuous-time semi-distributed model which integrates hydrological processes, vegetation and crop growth, erosion, and nutrient dynamics at the catchment scale. It is based on two previously developed tools: SWAT (Arnold *et al.* 1993) and MATSALU (Krysanova *et al.* 1989). SWIM was used in this study as it fulfils the requirements of data availability and distributed character. Moreover, it enables the estimation of the soil moisture content in several soil layers and has its own geographic information system (GIS) interface.

SWIM is spatially disaggregated into a three-level scheme: basin, subbasin and hydrotope. The hydrotope is a spatial unit of unique geographical properties and therefore it may be assumed to be a unit of uniform hydrological response and nutrient cycle behaviour. Hydrotopes are derived by means of the GIS tools by overlaying three input layers: the map of land use, the soil map, and the map of subbasins.

This physically based model includes calculations of the individual hydrological processes following specific techniques: the water percolation–storage routing technique based on the Simulator for Water Resources in Rural Basins (SWRRB) (Arnold *et al.* 1990), the direct runoff–Soil Conservation Service–Curve Number (SCS CN) technique, subsurface lateral flow (details are given in the following paragraph), groundwater recharge (Sangrey *et al.* 1984), evapotranspiration (Priestley & Taylor 1972; Ritchie 1972), vegetation cycle (Williams *et al.* 1984), snowmelt–degree day method (Knisel 1980), and river routing (Muskingum routing). All processes are calculated for each hydrotope in a daily step and then aggregated for the particular subbasin. A detailed description of the model can be found in Krysanova *et al.* (1998, 2005). SWIM proved to be a suitable tool for the simulations of the hydrological cycle in Central Europe (Hattermann *et al.* 2005; Nemeckova *et al.* 2011). The total runoff from the area is calculated as the sum of three components: direct runoff (in terms of SCS CN), subsurface lateral flow, and groundwater runoff.

There are two possible ways to calculate lateral subsurface flow in SWIM. The term ‘lateral subsurface flow’, or ‘interflow’, represents the contribution of the streamflow which originates below the surface, but above the zone where rocks are saturated with water. The first one is given by the exponential storage routing technique (hereinafter called the SWRRB approach) of Arnold *et al.* (1990), which originates from the Simulator for Water Resources in Rural Basins (SWRRB; Williams *et al.* 1985), based on the following relation:

$$SSF = (SW_{(i)} - FC) \left[ 1 - \exp\left(\frac{-\Delta t}{TT}\right) \right] \quad (1)$$

where  $SW_{(i)}$  is the soil water content on day  $i$  (mm),  $FC$  represents the field capacity of the layer (mm), and  $TT$  the travel time through the layer (hrs).

The second possibility, given by the kinematic storage model (Sloan & Moore 1984) and used in the SWAT model, is expressed by the following relation:

$$SSF = 0.024 \left( \frac{2(SW_{(i)} - FC)K_{sat}slp}{\varphi_d L_{hill}} \right) \quad (2)$$

where  $K_{sat}$  denotes the saturated hydraulic conductivity ( $\text{mm h}^{-1}$ ),  $slp$  is the average slope of the hydrotope ( $\text{m m}^{-1}$ ),  $\varphi_d$  represents the drainable porosity ( $\text{mm mm}^{-1}$ ), and  $L_{hill}$  the hillslope length (m).

The daily sum of precipitation, air temperatures (minimum, maximum, and average), relative humidity, and solar radiation represent the inputs into SWIM. The wind speed is optional.

## RESULTS

### Discharge calibration and validation

The original version of SWIM has 17 calibration parameters. The sensitivity analysis and description of most of these parameters may be found in Hattermann *et al.* (2005). The automatic parameter estimation algorithm (PEST) was chosen as a calibration tool. A detailed description of the PEST algorithm can be found in Doherty (2004).

The advantage of this method consists in the automaticity of the calibration process, especially when SWIM requires a number of parameters to be calibrated. The objective function is represented by a sum of squared weighted residuals. The model calibration was conducted separately for two lateral flow calculation techniques (kinematic storage and SWRRB) using the daily time step. Hence, two model set-ups (one using SWRRB and the second using the kinematic storage lateral flow estimation technique) were compared. The calibration period consisted of a 2-year period (2007–2008) and the validation period was represented by the following 2 years (2009–2010). The validation period was extracted from a continuous simulation (starting in 2007) using the entire calibration period to set-up initial hydrologic conditions. In the validation period, the soil moisture content as well as groundwater level measurements were available.

Values of the Nash–Sutcliffe index of performance (NS) of 0.44 (using the kinematic storage method) and 0.33 (using the SWRRB storage routing method) were obtained for the entire calibration period (2007–2008) at a daily time step. The selected calibration parameters are shown in Table 2 (four parameters concerning initial hydrologic conditions and four routing parameters are omitted). The model efficiency in the validation period (2009–2010) was lower, attaining 0.21 (kinematic storage method) and 0.22

(SWRRB approach). The model performance in both periods is shown in Figure 2. The error statistics of discharge simulations concerning both calibration and validation periods are shown in Table 3. The table demonstrates very similar performances of the two model set-ups. However, with regard to the water balance (average simulated discharge compared to average observed discharge), the kinematic storage model performed significantly better than the exponential storage routing approach (SWRRB). The SWRRB model set-up significantly underestimated runoff volume. As shown in Figure 2, the kinematic storage method also outperformed SWRRB in capturing flood events. In the entire period of interest (2007–2010), seven runoff episodes exceeded the discharge of  $0.05 \text{ m}^3 \text{ s}^{-1}$  (approximately five times the average long-term average). Peak discharges of these episodes were underestimated on average by 75% (SWRRB) and 41% (kinematic storage). The particular runoff components (for both model set-ups) are displayed in Table 4 for the validation period (2009–2010). Almost no direct runoff was observed in both modelling approaches. This is the result of the highly permeable soil and thus a low SCS curve number (ranging from 35 to 40 according to the antecedent wetness). The main difference between the two modelling approaches is the amount of subsurface lateral flow generated. The kinematic storage approach generated 183 mm of subsurface lateral flow in 2 years (2009–2010), whereas the SWRRB approach generated 23 mm. Hence, the kinematic storage approach enabled a significantly higher portion of runoff to be generated in the soil profile than SWRRB. In the SWRRB model set-up, water was generally more prone to percolate to groundwater, which then represented the main runoff component.

Simulated yearly values of actual evapotranspiration ranged from 450 to 600 mm with annual averages of 500 and 525 mm, depending on the model set-up. These values correspond to the acceptable range (Greminger 1984) and are only slightly higher than those observed by Tuzinsky (2002).

The error statistics demonstrated the fact that SWIM is not a suitable tool to simulate discharge in such a small-scale area. Although it is able to simulate the response of the catchment to rainfall, the recession curves are estimated inadequately. The main discrepancies between observed and

**Table 2** | The values of selected model parameters concerning both lateral flow modelling techniques

Parameter	Units	Kinematic storage	SWRRB
Evapotranspiration correction on sky emissivity	[-]	0.99	0.98
Base flow factor – return flow travel time	[-]	0.95	0.97
Groundwater recession	[-]	0.50	0.83
Groundwater delay	[day]	185.00	99.44
Temperature of snowfall	[°C]	0.50	0.50
Temperature of snowmelt	[°C]	0.00	0.00
Snowmelt rate	[mm day <sup>-1</sup> ]	0.26	0.26
Correction of saturated hydraulic conductivity	[-]	0.50	0.46
Correction of winter precipitation amount	[-]	1.15	1.06

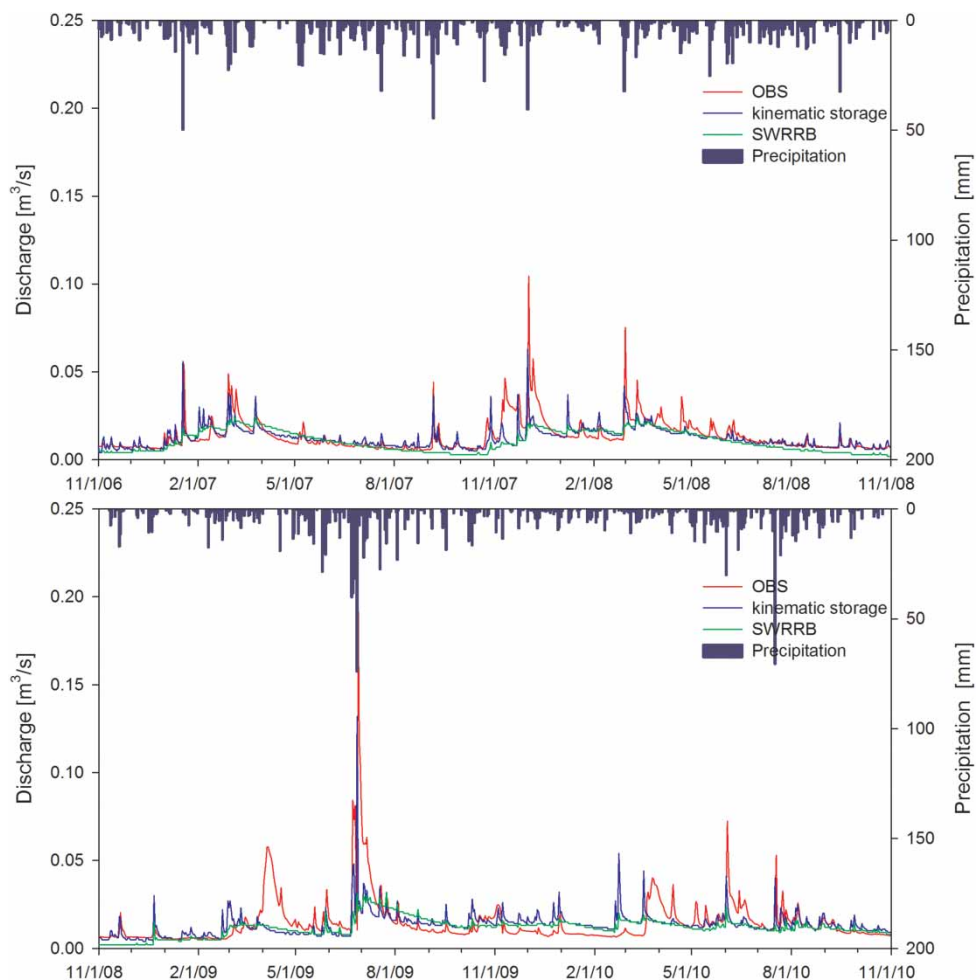


**Figure 2** | Discharge simulation in the years 2007–2010 using the kinematic storage method and the SWRRB technique for the Liz gauging station.

**Table 3** | The error statistics of the model performance concerning discharge simulation for the entire calibration (2007–2008) and validation (2009–2010) periods

	Kinematic storage		SWRRB	
	Calibration	Validation	Calibration	Validation
NS [-]	0.44	0.21	0.33	0.22
RMSE [ $\text{m}^3 \text{s}^{-1}$ ]	0.007	0.013	0.008	0.013
RE [%]	65	122	71	116
$R$ [-]	0.64	0.46	0.61	0.49
B [%]	-8.1	-7.9	-20.9	-19.5

NS – Nash–Sutcliffe index; RMSE – root mean square error: the average square difference between observed and modelled discharge; RE – relative error: root mean square error divided by the observed average discharge;  $R$  – correlation coefficient; B – difference between the average observed and modelled discharges.

simulated discharges might be explained by an inaccurate estimation of the snowmelt process. Nevertheless, the

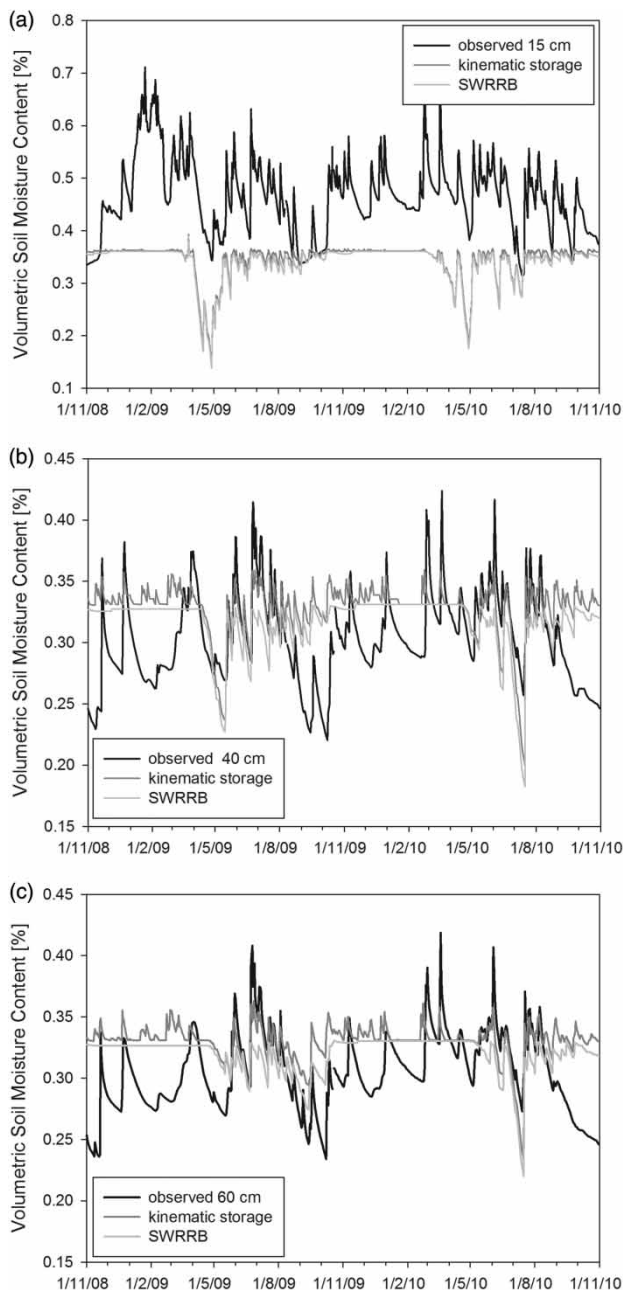
kinematic storage lateral flow estimation approach represents a more efficient opportunity to simulate discharge in the small-scale forested catchment compared to the SWRRB approach (particularly with regard to the long-term water balance and high-flow episodes).

### Soil moisture simulations

The simulation of soil moisture dynamics in the Liz catchment was evaluated in the hydrologic years 2009–2010. The influence of two different lateral flow estimation approaches was assessed. The measured and simulated values are displayed in Figure 3 for three different layers (15, 40, and 60 cm). The yearly course of soil moisture can be divided into two distinct periods. Wintertime is

**Table 4** | The average yearly values of runoff components [mm] in the validation period (2009–2010)

Lateral flow approach	Precipitation	Direct runoff	Lateral flow	Groundwater flow	Actual evapotranspiration
SWRRB	916	0	12	363	484
Kinematic storage	916	3	92	343	482

**Figure 3** | Simulated and observed soil moisture content at depths of (a) 15, (b) 40, and (c) 60 cm (2009–2010).

accompanied by an increase in the soil moisture content after the warmer and dryer part of the year. This increase is regularly interrupted by declines of the moisture content with obviously slower dynamics than the drops during the summer and autumn, probably caused by substantially lower values of transpiration. Winter declines of the moisture content exhibit an undisturbed character, as prevailing precipitation amounts are in the form of snow and therefore do not infiltrate directly into the soil profile. The refilling of the soil profile is possible only in the case of temperatures above zero and the presence of snow or rainfall. In contrast, fluctuations in the soil moisture content during a summer period exhibit a more complex pattern, which can be generally characterized by a slow reduction resulting in the minimum saturation during autumn. The seasonal dynamics follow a similar seasonal pattern in all layers.

Based on the observed character of soil moisture dynamics the year was split into warm and cold periods. The warm period was defined as 1 April to 31 August, and therefore nearly coincides with the vegetation period (from 1 May to 7 October) defined by Tesař *et al.* (2001). The colder period spans from the beginning of September to the end of March.

According to Figure 3(a), the simulated water content at the depth of 15 cm was significantly underestimated by the model and the mean value would always be a better estimate (Table 5). This is caused either by the influence of hysteresis or by the extremely variable porosity present in the top soil layer. Hence, in this top layer it is better to assess only the dynamics of the water content. However, it did not comply satisfactorily with the modelled values on the yearly basis. Only in the case of summer and autumn periods were there several similarities (Figure 3(a)). The detailed statistics in Table 6 show that both modelling approaches had very similar results in terms of root mean square error (RMSE), correlation coefficient, and soil water balance.

**Table 5** | The Nash–Sutcliffe coefficients concerning soil moisture simulations in the various soil layers and for the entire soil profile (total soil moisture content (SMC)) in the validation period 2009–2010

Period	Lateral flow	15 cm	40 cm	60 cm	Total SMC
Cold 2009	Kinematic storage	-0.79	-1.82	-2.92	-0.80
	SWRRRB	-0.82	-1.04	-1.68	-0.64
Warm 2009	Kinematic storage	-4.56	0.44	0.33	0.62
	SWRRRB	-5.33	0.15	0.15	0.35
Cold 2010	Kinematic storage	-2.51	-0.72	-0.40	-0.36
	SWRRRB	-2.62	-0.31	0.16	-0.04
Warm 2010	Kinematic storage	-5.13	-0.04	0.07	0.37
	SWRRRB	-5.75	-0.70	-0.45	-0.05

For the depth of 40 cm, the model performance was slightly more reliable than in the case of 15 cm, as documented, for example, by the total predicted soil water volume (Table 6) or Nash–Sutcliffe coefficient (Table 5). According to Figure 3(b), the model simulation was again more satisfactory in the warmer period of the year. The most obvious discrepancies were connected with winter soil moisture declines that were not estimated at all. Hence, in the winter period the use of the mean value would be more efficient (Table 5). The SWRRRB lateral flow model set-up estimated the soil moisture balance better and the kinematic storage approach gave higher correlations and a more efficient NS index (in the warm season).

The model performance in the last layer measured by the tensiometer (60 cm) is shown in Figure 3(c). It exhibited behaviour similar to that in the above layer. Even the amplitude of the soil water content curve was close to that of the adjacent layer, implying that the soil within these two depths acts as one homogenous unit, at least from a soil moisture point of view. The only difference from the previous soil layer is represented by the correlation coefficient between the observed and simulated data (Table 6), which is similar using both methods studied (SWRRRB and kinematic storage).

Finally, the moisture content of the entire soil profile was compared with the measurements. The average monthly values of the soil moisture content (2009–2010) exhibited similar trends to the values of runoff (Figure 4), with the minimum values in September and October and a double maximum (in March and June), the first one caused by snowmelt, the second by summer rainfall. The moisture content was estimated satisfactorily during the

**Table 6** | The performance of soil moisture simulations in the various soil layers in the validation period 2009–2010 (notation defined in the caption of Table 2)

Depth	Lateral flow	RMSE [ $\text{cm}^3 \text{cm}^{-3}$ ]	R [-]	Balance [%]
15 cm	Kinematic storage	0.136	0.25	-24.7
	SWRRRB	0.141	0.27	-25.9
40 cm	Kinematic storage	0.046	0.27	8.2
	SWRRRB	0.042	0.19	4.4
60 cm	Kinematic storage	0.040	0.35	7.2
	SWRRRB	0.035	0.32	4.2
Total SMC	Kinematic storage	0.034	0.51	4.5
	SWRRRB	0.033	0.42	2.1

SMC – soil moisture content.

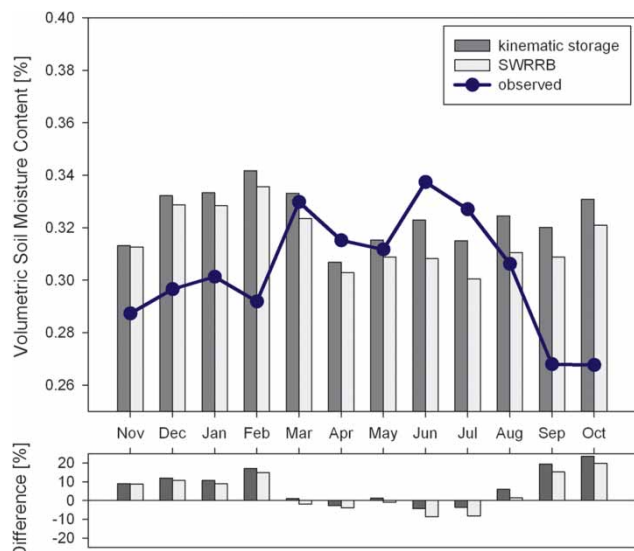


**Figure 4** | Comparison of the simulated and observed monthly average soil moisture contents in the Liz catchment (2009–2010).

warm season (Figure 4). On the contrary, the model estimates seemed to be less satisfying during the cold period. Hence, for more detailed investigation of the results, the year was split into two distinct parts more or less corresponding to the vegetation and non-vegetation seasons (as defined above).

The model simulations in the cold period compared to the observed data are shown in Figure 5. This comparison demonstrates that the model routines used for the soil water content estimation have a limited ability to predict the winter moisture fluctuations in the case of the Liz catchment. The main difference is in the inability to simulate the depletion of the soil moisture content that takes place in the



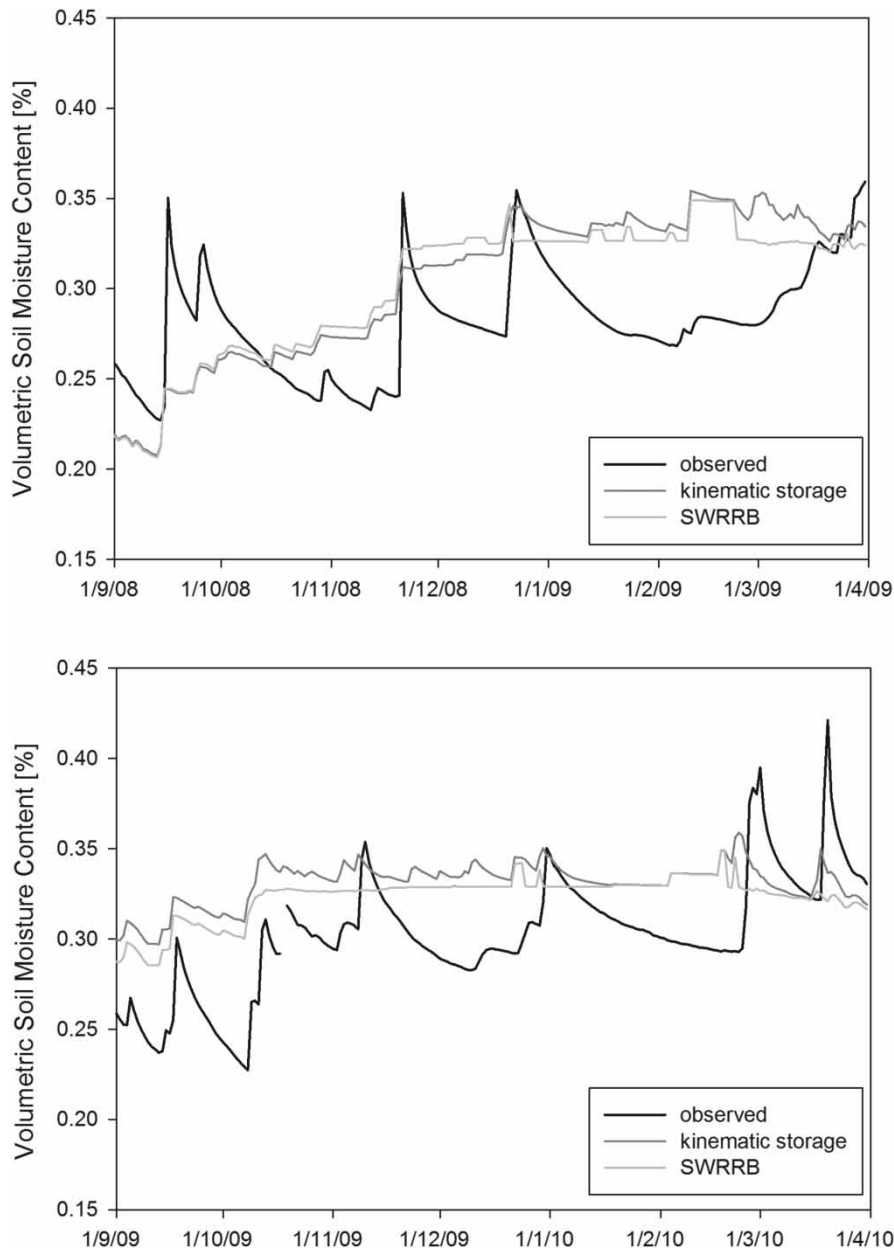


**Figure 5** | Model performance of the total soil moisture content simulation in the cold season (1 September–31 March).

non-precipitation periods. The simulated values generally corresponded to the observed ones only after a period of significant rainfall or snowmelt. The corresponding statistics are shown in Table 7. The correlation coefficient values of both methods generally oscillated between 0.50 and 0.55 in both winter periods (Figure 6). The average modelled soil water content was overestimated by approximately 8 and 7% in 2009 and 10 and 7% in 2010 depending on the

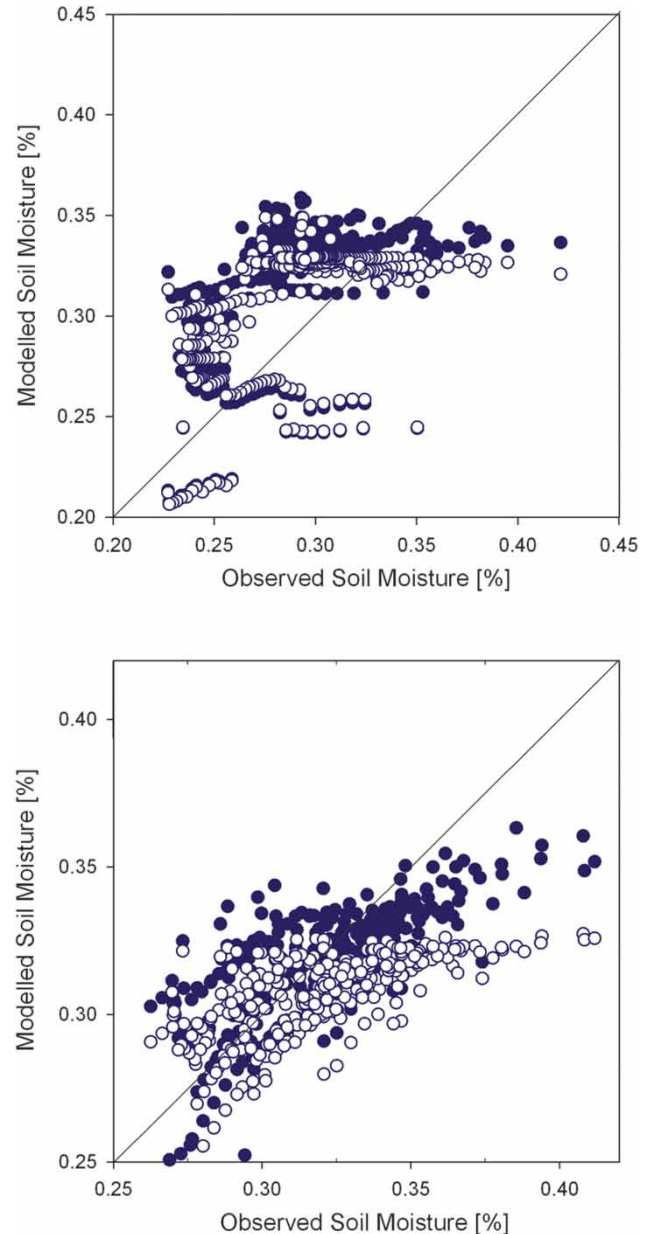
lateral flow technique used. The RMSE did not differ substantially between the two techniques applied and oscillated between 0.035 and 0.045 of the total soil moisture content. Generally, the modelled values were able to describe the main process of refilling of the soil moisture content during the cold season. Nevertheless, both modelling approaches failed to predict the declines of the moisture content, which might be a result, for example, of

**Table 7** | The seasonal error statistics of the total (entire soil column SMC) soil moisture simulations (notation defined in the caption of Table 2)

Period	Lateral flow	RMSE [cm <sup>3</sup> cm <sup>-3</sup> ]	R [-]	Balance [%]
Cold 2009	Kinematic storage	0.042	0.52	7.8
	SWRRB	0.041	0.48	7.2
Warm 2009	Kinematic storage	0.020	0.83	0.4
	SWRRB	0.026	0.77	-3.4
Cold 2010	Kinematic storage	0.041	0.53	9.5
	SWRRB	0.035	0.54	7.0
Warm 2010	Kinematic storage	0.019	0.68	-1.9
	SWRRB	0.025	0.63	-4.9

a gradual percolation to lower layers of the soil profile or evapotranspiration losses (Moore *et al.* 2011).

The model simulation in the warm period of 2009–2010 is depicted in Figure 7. The correlation coefficients were significantly higher compared to the cold season and equalled 0.83 for 2009 and 0.68 for 2010 in the case of the kinematic storage technique. The SWRRB approach attained values of 0.77 and 0.63 for the summers of 2009 and 2010, respectively. Considering both model set-ups, the correlation coefficient for the year 2010 was lower due to the minor shift between the simulated and observed data at the beginning of the season. However, the fluctuations and their magnitudes were represented satisfactorily. Contrasting the warm and cold periods, the total soil moisture content was estimated with a high level of accuracy in summertime. The differences between the mean observed and simulated values did not exceed 2 and 5% with the kinematic storage model and the SWRRB technique (see Table 7), respectively. The average soil moisture content for individual months is depicted in Figure 4. This gives good modelling performance from March to August. The RMSE was also generally better than in the cold period, ranging from 0.02 to 0.03. The NS index (Table 7) documents a better efficiency of the kinematic storage model set-up in the warm period. It attains values of 0.62 (2009) and 0.37 (2010), compared to 0.35 (2009) and -0.05 (2010) using the SWRRB technique. The kinematic storage also performed more efficiently from the point of view of the soil moisture balance, RMSE, and correlation coefficient (Table 7). In conclusion, the rises and declines in the moisture content

**Figure 6** | Comparison of the simulated and observed daily soil moisture in the Liz catchment in the cold season (upper panel) and warm season (lower panel). Kinematic approach – dark circles; SWRRB – white circles.

and the low soil moisture values were predicted reasonably well during this period. Only maximum saturation periods were slightly underestimated by the model. This might be caused by the daily time step and also by the heterogeneity of the soil characteristics. Moreover, the influence of the single retention curve causes a slight overestimation of high soil moisture contents in soil.

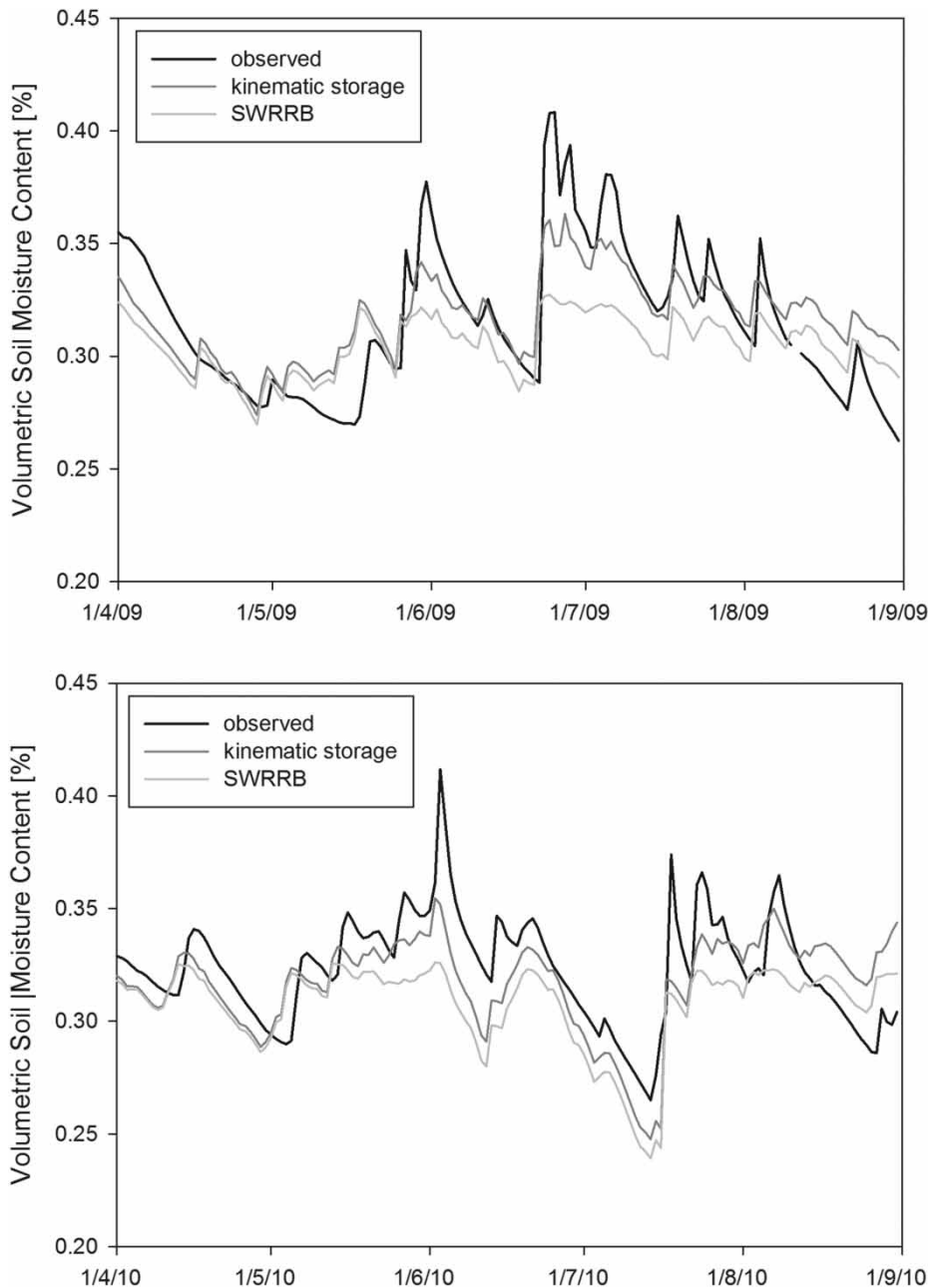


**Figure 7** | Model performance for the total soil moisture content in the warm season (1 April–31 August).

### Groundwater level simulations

The efficiency of the groundwater module of SWIM was assessed for the entire period of the available data (2007–2010). The simulated daily values of the groundwater level are compared to available weekly observations. In the period of 2007–2010, only four measurements are missing.

The results of simulation by both model set-ups (kinematic storage and SWRRB lateral flow estimation) are contrasted with observations in [Figure 8](#). The figure demonstrates the different abilities of the two modelling approaches to estimate the seasonal course of the groundwater level. Focussing on the recession curves, the kinematic storage approach was more reliable in the estimation of their

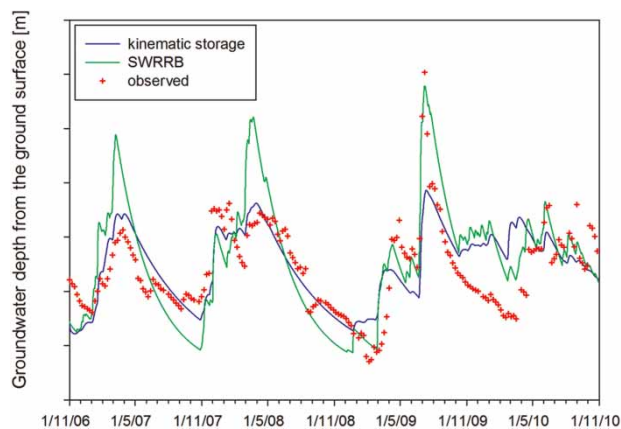


**Figure 8** | The observed and simulated groundwater level in the years 2007–2010.

shape compared to the SWRRB approach, which tended to produce quicker recessions. According to the error statistics, the kinematic storage method was more efficient in terms of groundwater balance (kinematic storage: +1.2%; SWRRB: +2.9%, compared to observed values) and relative error (kinematic storage: 11.2%; SWRRB: 13.4%). Contrarily, the SWRRB approach attained higher values of the correlation coefficient with the observed values (0.75 compared to 0.66 with the kinematic storage method).

Groundwater level simulations documented the ability of the hydrological model to capture its fundamental fluctuations in the small-scale catchment. Based on the error statistics (with the exception of the correlation coefficient) and the recession curve shape, the kinematic storage model set-up represented the more reliable option.

## DISCUSSION

The ecohydrological model SWIM, which has generally very similar hydrological components to the well-established SWAT model, proved to have limited or no ability to simulate the discharge in the small-scale Liz experimental catchment. The results of discharge simulations are worse than those acquired from the SWAT model simulations in small agricultural catchments by *Srinivasan et al. (2005)* and *Kannan et al. (2007)*, but they outperform the simulations by *Spruill et al. (2000)*; however, in this work a karst-influenced catchment has been studied. The poor model performance concerning discharge simulations is

caused by a combined effect of several issues. First, the winter inconsistency between observed and simulated discharges is determined by a complex character of the snowmelt process. The most pronounced difference is in April 2009 when snow has not started to melt until the temperature of 5 °C was exceeded (the snowmelt threshold is usually slightly above 0 °C). Hence, the simple degree day method (used in this version of SWIM) is not always able to capture the dynamics of snowmelt in forest. Variable parameters of the degree day method or different snowmelt method would be beneficial. Second, a possible source of uncertainty for forested plots is represented by the rate of interception. SWIM allows it to be varied according to the leaf area index to a maximum value of 2.5 mm, which is less than the observed 4.8 mm (*Dohnal et al. 2014*). Only if the SCS CN curves technique is activated will the interception exceed this threshold. Moreover, coniferous forest might intercept even more precipitation in the form of snow in the winter period (*Šípek & Tesar 2014*) and therefore modify the runoff response to precipitation. On the contrary, the influence of deposited precipitation (originating from fog), which might add approximately 7% to the total annual vertical precipitation in this region (*Elias & Tesar 1994*), was neglected. These first two points stress the uncertainty concerning the precipitation inputs in the forested plot. Finally, the rainfall–runoff relation in the area might be more complicated than described by the model design. For example, the introduction of macropore flow (as a fourth source runoff) might help to better estimate the reaction of the forested area to rainfall. The need for another source of runoff is indicated by shapes of simulated recession curves (see *Figure 2*), which do not always follow observed discharges (especially following high-flow periods).

The soil moisture simulations exhibited contrasting results. The yearly course of simulation was therefore divided into two distinct periods according to the model efficiency. First, in the warmer part of the year (April–August), the dynamics of the total soil moisture content are simulated quite accurately. The minimum and maximum values are predicted well and only peak values of the moisture content are slightly underestimated, which might be caused by the daily time step of the model. The results from this period are comparable to those obtained

by Li *et al.* (2010) using the SWAT model in China or DeLiberty & Legates (2003), who used the SWAT model for soil moisture simulations in Oklahoma, USA. The results for the summer are only slightly worse than the soil moisture simulations performed by another type of model dealing explicitly with soil moisture accounting (Brocca *et al.* 2008; Chen *et al.* 2014). Secondly, in the colder part of the year the dynamics of soil moisture seem to be represented inadequately by the model. Although the main process of soil moisture content refilling is observed. These declines might be explained by winter transpiration (Moore *et al.* 2011) or by percolation to deeper layers. The depth distribution of the moisture content is simulated poorly in the entire year. Moreover, the function of the field capacity concept recorded in this particular layer is problematic, as the water is drained just after moisture reaches the threshold value. Hence, no significantly higher values of simulated soil moisture content are observed.

The groundwater level estimation using the kinematic storage lateral flow approach confirms that the groundwater module in SWIM is able to reproduce the observed water table dynamics in the small-scale forested catchment satisfactorily enough to serve as the lower boundary condition for plant water uptake. The results from the SWRRB approach are less satisfactory as the fluctuations of the groundwater level are significantly higher than the observed ones. This is caused by the model calibration with respect to discharge and the nature of both lateral flow estimation approaches. As no direct runoff is observed, total runoff is generated only by subsurface lateral flow and groundwater runoff. As the SWRRB approach generates only a small portion of subsurface lateral flow compared to the kinematic storage approach (Table 3), the groundwater is the key runoff component and therefore its fluctuation has to correspond closely to observed discharge. However, the runoff from the area partially originates from the soil profile (Cislerova 2005), and the observed groundwater fluctuations are less pronounced (Figure 8). The kinematic storage approach is therefore more suitable for hydrological modelling in mountainous areas with highly permeable soils, where a significant contribution of subsurface lateral flow might be expected.

## CONCLUSIONS

The aim of this study was to examine the ability of the mesoscale ecohydrological model SWIM to simulate the rainfall–runoff relationship within a small-scale forested mountainous catchment. In addition, a comparison of two different approaches of lateral flow estimation was performed.

SWIM has a limited ability to estimate the discharge in a small-scale forested catchment. This is probably caused by a larger uncertainty concerning precipitation inputs (interception and snowmelt process) compared to rural areas, variable soil hydraulic characteristics, and also by the character of the rainfall–runoff relation (significance of subsurface lateral flow). Estimates of the total soil moisture content in the forested area simulated by this type of hydrologic model are reliable only in the warm part of the year. The values of the soil moisture content should be dealt with carefully in the winter season as there are certain periods when they are significantly overestimated. The depth distribution of the soil moisture in particular soil layers is also not described well by the model. The observed uncertainty of the soil moisture simulation in the winter period and its year-round depth distribution represent main outcomes of the presented study. The fluctuations of the groundwater level were estimated sufficiently well.

The kinematic storage subsurface lateral flow estimation proved to be superior to the SWRRB approach, especially because of its ability to generate more subsurface lateral flow (which is a significant runoff component in forested mountainous catchments). This is even more important when soil is highly permeable and the SCS curve number (which is an inherent part of the model) does not allow direct runoff to be generated.

The results are especially valuable for modellers who wish to thoroughly describe the year-round hydrological cycle in landscapes with diverse land cover. This also includes the studies concerning the impact of climate and land-use changes on water resources. Further research will be focussed on the rate of evapotranspiration in the winter period as well as on the mechanism responsible for the soil water percolation. Furthermore, the possible introduction of new correction factors for the soil parameters will

be a topic of interest. This is crucial, because even measured values of hydrologic soil parameters might encounter errors, which may significantly influence the behaviour of the soil water content calculation.

## ACKNOWLEDGEMENT

The research was supported by the Technology Agency of the Czech Republic (TA02021451).

## REFERENCES

- Abbott, M. B., Bathurst, J. C., Cunge, J. A., O'Connell, P. E. & Rasmussen, J. 1986 An introduction to the European Hydrological System – Système Hydrologique Européen, SHE. 2. Structure of a physically-based, distributed modelling system. *J. Hydrol.* **87**, 61–77.
- Arnold, J. G., Williams, J. R., Nicks, A. D. & Sammons, N. B. 1990 *SWRRB – A Basin Scale Simulation Model for Soil and Water Resources Management*. Texas A&M University Press, College Station.
- Arnold, J. G., Allen, P. M. & Bernhardt, A. 1993 A comprehensive surface-groundwater flow model. *J. Hydrol.* **142**, 47–69.
- Beven, K. J. & Kirkby, M. J. 1979 A physically based, variable contributing area model of basin hydrology. *Hydrol. Sci. Bull.* **24**, 43–69.
- Brocca, L., Melone, F. & Moramarco, T. 2008 On the estimation of antecedent wetness conditions in rainfall–runoff modelling. *Hydrol. Process.* **22**, 629–642.
- Chen, M., Willgoose, G. R. & Saco, P. M. 2014 Spatial prediction of temporal soil moisture dynamics using HYDRUS-1D. *Hydrol. Process.* **28**, 171–185.
- Císlerová, M. 2005 Preferenční proudění ve vadózní zóně kambizemí. In: *Hydrologie malého povodí 2005* (M. Šir, L. Lichner, M. Tesar & L. Holko, eds). Institute of Hydrodynamics, AS CR, Prague, Czech Republic, pp. 23–30 (in Czech).
- Daly, E. & Porporato, A. 2005 A review of soil moisture dynamics: from rainfall infiltration to ecosystem response. *Environ. Eng. Sci.* **22**, 9–24.
- DeLiberty, T. L. & Legates, D. R. 2003 Interannual and seasonal variability of modelled soil moisture in Oklahoma. *Int. J. Climatol.* **23**, 1057–1086.
- Doherty, J. 2004 *PEST Model-Independent Parameter Estimation. User Manual*. 5th edn. Watermark Numerical Computing, Brisbane.
- Dohnal, M., Cerny, T., Votrubova, J. & Tesar, M. 2014 Rainfall interception and spatial variability of throughfall in spruce stand. *J. Hydrol. Hydromech.* **62**, 277–272.
- Elias, V. & Tesar, M. 1994 Horizontal precipitation: the input important from hydrological and ecological point of view. *J. Hydrol. Hydromech.* **42**, 105–114.
- Entin, J. K., Robock, A., Vinnikov, K. Y., Hollinger, S. E., Liu, S. X. & Namkhani, A. 2000 Temporal and spatial scales of observed soil moisture variations in the extratropics. *J. Geophys. Res.* **105**, 11865–11877.
- Fang, X., Ren, L., Li, Q., Liu, X., Yuan, F., Zhao, D. & Zhu, Q. 2012 Estimating and validating basin-scale actual evapotranspiration using MODIS images and hydrologic models. *Hydrol. Res.* **43** (1/2), 156–166.
- Ficklin, D., Luo, Y., Luedeling, E. & Zhang, M. 2009 Climate change sensitivity assessment of a highly agricultural watershed using SWAT. *J. Hydrol.* **374**, 16–29.
- Greminger, P. 1984 Physikalisch-ökologische Standortsuntersuchung über den Wasserhaushalt im offenen Sickersystem Boden unter Vegetation am Hang. *Mitteil. Eidgen. Anstalt Forstl. Versuchs.* **60**, 149–301.
- Hesse, C., Krysanova, V. & Hattermann, F. 2008 Eco-hydrological modelling in a highly regulated lowland catchment to find measures for improving water quality. *Ecol. Model.* **218**, 135–148.
- Hattermann, F., Krysanova, V., Wechsung, F. & Wattenbach, M. 2005 Runoff simulations on the macroscale with the ecohydrological model SWIM in the Elbe catchment – validation and uncertainty analysis. *Hydrol. Process.* **19**, 693–714.
- Holsten, A., Vetter, T., Vohland, K. & Krysanova, V. 2009 Impact of climate change on soil moisture dynamics in Brandenburg with a focus on nature conservation areas. *Ecol. Model.* **220**, 2076–2087.
- Huang, S., Hesse, C., Krysanova, V. & Hattermann, F. F. 2009 From meso- to macro-scale dynamic water quality modelling for the assessment of land use change scenarios. *Ecol. Model.* **220**, 2543–2558.
- Huang, S., Krysanova, V., Österle, H. & Hattermann, F. F. 2010 Simulation of spatiotemporal dynamics of water fluxes in Germany under climate change. *Hydrol. Process.* **24**, 3289–3306.
- Kannan, N., White, S. M., Worrall, F. & Whelan, M. J. 2007 Sensitivity analysis and identification of the best evapotranspiration and runoff options for hydrological modelling in SWAT-2000. *J. Hydrol.* **334**, 64–72.
- Knisel, W. G. 1980 *CREAMS: A field scale model for chemicals, runoff, and erosion from agricultural management systems*. USDA Conservation Research Report, 26, p. 643.
- Koch, S., Bauwe, A. & Lennartz, B. 2013 Application of the SWAT model for a tile-drained lowland catchment in north-eastern Germany on subbasin scale. *Water Resour. Manage.* **27**, 791–805.
- Krysanova, V., Meiner, A., Roosaare, J. & Vasilyev, A. 1989 Simulation modeling of the coastal waters pollution from agricultural watershed. *Ecol. Model.* **49**, 7–29.
- Krysanova, V., Becker, A. & Miller-Wohlfeil, D.-I. 1998 Development and test of a spatially distributed

- hydrological/water quality model for mesoscale watersheds. *Ecol. Model.* **106**, 261–289.
- Krysanova, V., Hattermann, F. & Wechsung, F. 2005 Development of the ecohydrological model SWIM for regional impact studies and vulnerability assessment. *Hydrol. Process.* **19**, 763–783.
- Li, M. X., Ma, Z. G. & Du, J. W. 2010 Regional soil moisture simulation for Shaanxi Province using SWAT model validation and trend analysis. *Sci. China Earth Sci.* **53**, 575–590.
- Moore, G. W., Bond, B. J. & Jones, J. A. 2011 A comparison of annual transpiration and productivity in monoculture and mixed-species Douglas-fir and red alder stands. *Forest Ecol. Manag.* **262**, 2263–2270.
- Nemeckova, S. 2008 *The Map of Soil Subtypes of the Czech Part of the Elbe River Basin for the Hydrological Model SWIM*. IH ASCR, Prague.
- Nemeckova, S., Slamova, R. & Šípek, V. 2011 Climate change impact assessment on various components of the hydrological regime of the Malše river basin. *J. Hydrol. Hydromech.* **59**, 131–143.
- Priestley, C. H. B. & Taylor, R. J. 1972 On the assessment of surface heat flux and evaporation using large scale parameters. *Mon. Weather Rev.* **100**, 81–92.
- Ritchie, J. T. 1972 A model for predicting evaporation from a row crop with incomplete cover. *Water Resour. Res.* **8**, 1204–1213.
- Sangrey, D. A., Harrop-Williams, K. O. & Kaliber, J. A. 1984 Predicting ground-water response to precipitation. *ASCE J. Geotech. Eng.* **110**, 957–975.
- Šípek, V. & Tesar, M. 2014 Seasonal snow accumulation in the mid-latitude forested catchment. *Biologia* **69**, 1562–1569.
- Sloan, P. G. & Moore, I. D. 1984 Modelling subsurface stormflow on steeply sloping forested watersheds. *Water Resour. Res.* **20**, 1815–1822.
- Spruill, C. A., Workman, S. R. & Taraba, J. L. 2000 Simulation of daily and monthly stream discharge from small watersheds using the SWAT model. *Trans. ASAE.* **46**, 1431–1439.
- Srinivasan, R., Ramanarayanan, T. S., Arnold, J. G. & Bednarz, S. T. 1998 Large area hydrologic modeling and assessment. Part II: model application. *J. Am. Water Resour. Assoc.* **34**, 91–101.
- Srinivasan, R., Gérard-Marchant, P., Veith, J. L., Gburek, W. J. & Steenhuis, T. S. 2005 Watershed scale modeling of critical source areas of runoff generation and phosphorus transport. *J. Am. Water Res. Assoc.* **41**, 361–377.
- Tesar, M., Šir, M., Syrovatka, O., Prazak, J., Lichner, L. & Kubik, F. 2001 Soil water regime in head water regions – observation, assessment and modelling. *J. Hydrol. Hydromech.* **49**, 355–375.
- Tuzinsky, L. 2002 Soil moisture in mountain spruce stand. *J. For. Sci.* **48**, 27–37.
- Van Genuchten, T. 1980 A closed-form equation for predicting the hydraulic conductivity of unsaturated soils. *Soil Sci. Soc. Am. J.* **44**, 892–898.
- Williams, J. R., Renard, K. G. & Dyke, P. T. 1984 EPIC – a new model for assessing erosion's effect on soil productivity. *J. Soil Water Conserv.* **38**, 381–383.
- Williams, J. R., Nicks, A. D. & Arnold, J. G. 1985 Simulator for water resources in rural basins. *J. Hydraul. Eng.* **6**, 970–986.

First received 10 December 2014; accepted in revised form 20 March 2015. Available online 28 April 2015